Title
Microfluidics platform for measurement of volume changes in immobilized intestinal enteroids

Journal
Biomicrofluidics, 8(2)

ISSN
1932-1058

Authors
Jin, Byung-Ju
Battula, Sailaja
Zachos, Nick
et al.

Publication Date
2014-03-01

DOI
10.1063/1.4870400

Peer reviewed

Microfluidics platform for measurement of volume changes in immobilized intestinal enteroids

Byung-Ju Jin,[1] Sailaja Battula,[1] Nick Zachos,[2] Olga Kovbasnjuk,[2] Jennifer Fawlke-Abel,[2] Julie In,[2] Mark Donowitz,[2] and Alan S. Verkman[1,a)]
[1]*Departments of Medicine and Physiology, University of California, San Francisco, California 94143, USA*
[2]*Departments of Physiology and Medicine, Gastroenterology Division, Johns Hopkins University School of Medicine, Baltimore, Maryland 21205, USA*

(Received 13 February 2014; accepted 24 March 2014; published online 1 April 2014)

Intestinal enteroids are *ex vivo* primary cultured single-layer epithelial cell spheroids of average diameter ~150 μm with luminal surface facing inward. Measurement of enteroid swelling in response to secretagogues has been applied to genetic testing in cystic fibrosis and evaluation of drug candidates for cystic fibrosis and secretory diarrheas. The current measurement method involves manual addition of drugs and solutions to enteroids embedded in a Matrigel matrix and estimation of volume changes from confocal images of fluorescently stained enteroids. We developed a microfluidics platform for efficient trapping and immobilization of enteroids for quantitative measurement of volume changes. Multiple enteroids are trapped in a "pinball machine-like" array of polydimethylsiloxane posts for measurement of volume changes in unlabeled enteroids by imaging of an extracellular, high-molecular weight fluorescent dye. Measurement accuracy was validated using slowly expanding air bubbles. The method was applied to measure swelling of mouse jejunal enteroids in response to an osmotic challenge and cholera toxin-induced chloride secretion. The microfluidics platform allows for parallel measurement of volume changes on multiple enteroids during continuous superfusion, without an immobilizing matrix, and for quantitative volume determination without chemical labeling or assumptions about enteroid shape changes during swelling. © *2014 AIP Publishing LLC*. [http://dx.doi.org/10.1063/1.4870400]

INTRODUCTION

Tissue spheroids and organoids comprised of normal or diseased cells have been used extensively to study cellular physiology and disease mechanisms, and to test therapeutics.[1,2] Recently, it has become possible to generate enteroids consisting of a single layer of intestinal epithelial cells (enterocytes) with the luminal (apical) surface facing inward.[3–6] Intestinal enteroids represent a significant advance in gastrointestinal physiology and medicine because it has not been possible to generate primary enterocyte cultures. An important application of intestinal enteroids is analysis of membrane transport phenomena, such as transepithelial fluid secretion driven by active sodium or chloride transport. Enteroids generated from human rectal biopsies from cystic fibrosis patients have been used to study the phenotype of mutant CFTR (cystic fibrosis transmembrane conductance regulator) chloride channels causing cystic fibrosis and the potential efficacy of CFTR-targeted drugs and gene therapy.[7,8] Another major transport application of enteroids is in studies of the pathophysiology of secretory diarrheas and testing of potential antisecretory therapeutics.[7–9]

[a)]Author to whom correspondence should be addressed. Electronic mail: Alan.Verkman@ucsf.edu. Tel.: 415 476-8530, Fax: 415 665-3847. URL: http/www.ucsf.edu/verkman

The principal readout in membrane transport studies is enteroid volume, which changes with osmotic water movement driven by active transepithelial ion or solute transport. The current approach to follow enteroid volume changes involves confocal imaging of enteroids in response to addition of membrane transport agonists or inhibitors, or changes in solution composition.[7] Enteroids are immobilized in an extracellular matrix such as Matrigel and images are acquired following manual solution changes. Limitations of the current methodology include: (i) restrictions of the embedding extracellular matrix on access of extracellular components and enteroid swelling; (ii) inefficient solution mixing; (iii) the need to label enteroids with a fluorescent dye for confocal imaging; (iv) challenges in making parallel measurements on many enteroids; and (v) inaccuracies in deducing enteroid volume changes from confocal images. The latter limitation is quite significant because of the anisotropic shape and swelling of enteroids, particularly when immobilized in an extracellular gel matrix.

In order to overcome these limitations, we developed a microfluidics platform to immobilize enteroids for efficient superfusion and continuous, parallel image acquisition without the need for an immobilizing matrix. Enteroid volume is deduced quantitatively from area-integrated fluorescence of an excluded extracellular dye, without the need for enteroid staining or assumptions about enteroid shape and swelling geometry. Applications are demonstrated for measurements of transepithelial osmotic water permeability and cholera toxin-induced fluid secretion.

EXPERIMENTAL

Microchannel fabrication

The microchannel was fabricated using conventional photolithography with mask, master, and PDMS (polydimethylsiloxane) stamp processes. The microchannel design (drawn using AUTOCAD 2010, Autodesk) was printed onto a film mask at 25 400 dpi resolution (CAD/Art Services, Inc.). To prepare the master with uniform height $>200\,\mu$m, SU-8 2075 negative photoresist (Microchem Corp.) was spin-coated onto a silicon wafer (Addison Ddison Engineering, Inc.) in two steps. In the first step, $\sim$4 ml SU-8 2075 was dropped on a 4-in. diameter silicon wafer and spin-coated at 500 rpm for 10 s and then at 2000 rpm for 30 s to give 110–120 μm thickness, and then prebaked at 65 °C for 5 min and at 95 °C for 30 min. The same procedure was repeated to give 220–240 μm final thickness. The photoresist was then exposed to UV light (350 nm, 280 mJ/cm^2 for 56 s) through the previously prepared film mask and post-baked at 65 °C for 5 min and then at 95 °C for 14 min. The final features on the silicon wafer were developed using SU-8 developer (MicroChem Corp.) for 30 min in a sonicator. The channel height of the master was measured as $\sim$240 μm using a profilometer (XP-2 stylus profilometer, Ambios Technology, Inc.).

The PDMS microchannel was fabricated by standard replica molding, using DA-184A and DA-184B (Dow Corning) in a 5:1 ratio. Liquid PDMS was poured on the master and air bubbles in the deep structure were eliminated under vacuum for 1 h, and cured at 80 °C for 1 h. The wafer was refrigerated at -20 °C for 2 h to shrink the microstructure before peeling the PDMS stamp from the silicon wafer in order to prevent disruption during peeling. The inlet and outlet of the PDMS stamp were punched with a 2-mm biopsy punch (Harris Uni-Core) and bonded onto a glass slide (Thermo Scientific Erie Scientific) using air plasma treatment (Harrick Plasma) at 700 mTorr for 50 s.

Trapping efficiency was determined as the number of the trapped enteroids divided by the total number of the injected enteroids.

Enteroid volume change measurement

Enteroid volume change was measured by imaging of an enteroid-excluded, extracellular fluorescent dye in which changes in enteroid volume alter the total amount of dye in the enteroid-containing area. To minimize scattering and shadow effects, a long-wavelength fluorescent dye (10000 dextran Alexa Fluor 647, Molecular Probes) was imaged using a 2$\times$ magnification lens (Nikon Plan UW, numerical aperture 0.06, working distance 7.5 mm) with $>250\,\mu$m depth-of-field. Enteroid volume was computed from area-integrated fluorescence as described in

results. To validate the accuracy of volume determination, slowly expanded bubbles are generated in the microfluidic chamber (see supplementary Fig. S1[10] and movie S1[10]) by injecting low-temperature (4 °C) cell culture media. Bubble volumes deduced by fluorescent dye exclusion were compared to volumes deduced by light microscopy assuming spherical geometry.

Experimental and computational visualization of flow pattern around microstructures

Experimental determination of flow pattern was accomplished by visualizing the streaklines of small fluorescent particles (diameter 7 μm, Bangs Laboratories, Inc.). Flow patterns were determined around unoccupied posts and posts occupied by large polystyrene beads (150 μm, Bangs Laboratories, Inc.).

Computational determination of the flow-field around microstructures, with and without trapped enteroids, was done by finite-element simulations using COMSOL Multiphysics (version 3.4; COMSOL). The Navier-Stokes solver for an incompressible fluid was used with ~200 000 mesh elements. Boundary conditions included constant-velocity at the inlet, and no viscous stress and pressure boundary at the outlet.

Enteroid culture

Mice (age 6–12 weeks, CD1 genetic background) were maintained in air-filtered cages and fed normal mouse chow in the UCSF. Animal Care facility. Procedures were approved by the UCSF Committee on Animal Research. Mice were sacrificed using high-dose avertin and the intestine was collected and placed in ice-cold PBS (Phosphate buffered saline). Crypts were isolated as described.[3,11] Briefly, the mid-jejunum (~7 cm) was opened lengthwise, and 3–5 mm cut fragments were washed and incubated for 1 h in chelation buffer (in mM: 5.6 Na_2HPO_4, 8.0 KH_2PO_4, 96.2 NaCl, 1.6 KCl, 43.4 sucrose, 54.9 D-sorbitol, and 0.5 dithiothreitol) containing 2 mM EDTA. Crypts were pelleted at 400 g for 10 min and plated by resuspending 200–300 crypts in 50 μl Matrigel (growth factor-reduced, phenol-free; BD Biosciences). Enteroids were cultured in DMEM (Dulbecco's modified Eagle's medium)/F12 containing 100 U/ml penicillin/streptomycin, 10 mM HEPES (4-(2-hydroxyethyl)-1-piperazineethanesulfonic acid), 2 mM Glutamax, 1:50 dilution B27 supplement, 1:100 dilution of N2 supplement (all from Invitrogen), 500 μM N-acetylcysteine (Sigma), 100 ng/ml Noggin (Peprotech), 50 ng/ml EGF (Epidermal growth factor, Sigma), 10 nM L-gastrin (Anaspec), 10 mM nicotinamide (Sigma), 500 nM A83 (Tocris), and 10 μM SB202 (Sigma). Wnt3A (50% final volume) and R-Spondin1 (20% final volume) were supplemented as conditioned media generated from transfected cells, as described.[11] The medium was changed every 2–3 days and the enteroids were passaged weekly. For passage, the Matrigel was disrupted using a P200 pipette in 1 ml of cell recovery solution (BD Biosciences) and by 20 min incubation at 4 °C on an orbital shaker. The enteroids were transferred to 15 ml Falcon tube, centrifuged at 400 g for 10 min at 4 °C, and the pellet was resuspended in Matrigel for plating.

Enteroid recovery for microfluidics studies

Enteroids at passage 4 or above were used to minimize villous fragments and tissue debris. Most of the enteroids became rounded within 1–2 days after splitting, as described.[3,11] The enteroids were recovered from Matrigel with cell recovery solution by 20-min incubation at 4 °C on an orbital shaker. Centrifugation was not done in the recovery procedure in order to prevent trauma to the enteroids. The enteroids were then added to advanced DMEM/F12 media containing 2 mM Glutamax and 10 mM HEPES and used for microfluidics studies within 3 h of harvesting.

RESULTS

Microfluidic chamber design

The design criteria for the microfluidic channel included efficient entrapment and immobilization of enteroids for continuous, parallel measurements on ten or more enteroids during

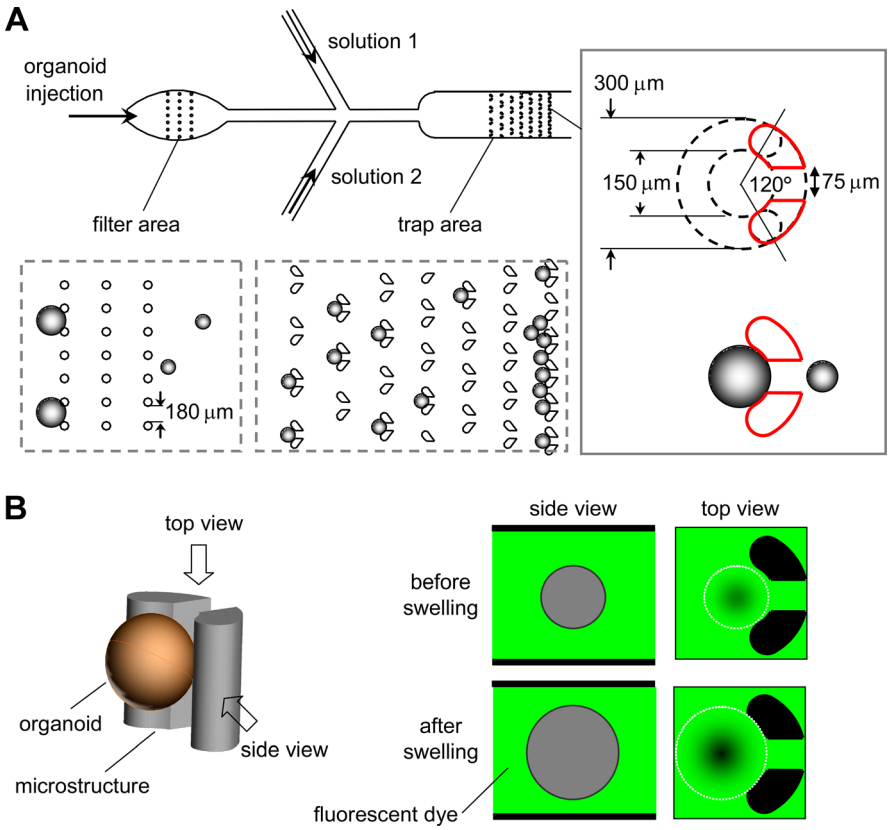

FIG. 1. Microfluidic channel design and volume measurement principle. (a) Channel design, showing passage of an enteroid suspension through a filter region to remove large particles and debris, and then into a trap region to immobilize for microscopy. Side injection ports allow continuous perfusion with different solutions. Inset at right shows post-pair geometry. (b) Principle of enteroid volume determination by fluorescent dye exclusion in which the perfusion solution contains a membrane-impermeant fluorescent dextran. Enteroid-excluded volume reduces area-integrated fluorescence signal.

perfusion. Additional criteria included rapid solution exchange, exclusion of very large or small enteroids in a heterogeneous population, prevention of clogging, and chamber reusability. As a major intended application is measurement of enteroid swelling, the design criteria also included a microscopy approach for continuous measurement of enteroid volume without assumptions about enteroid 3-dimensional geometry or shape changes during swelling or the need for fluorescent labeling of enteroids.

Fig. 1(a) diagrams the microfluidic channel design. A suspension of enteroids containing a heterogeneous size population is injected into the chamber. A filter region, consisting of a rectangular array of posts (100-μm diameter, 180-μm gap) traps large debris and very large enteroids to prevent clogging of the trap region. The trap region consists of rows of progressively more tightly spaced post-pairs to trap enteroids, with the final row closely spaced to trap all remaining enteroids for determination of trapping efficiency. The detailed geometry of the post-pairs shown in the figure inset was established empirically, after testing various shapes, to best immobilize individual enteroids during continuous perfusion and, for chamber reuse, to release them by reversal of perfusion direction. The gap in the post-pairs determines the minimum size of enteroids that are trapped, which can be tailored for enteroids of different sizes. The microfluidic channel design included two injection side-ports for solution exchange. The height of the trap area was $\sim$240 μm to minimize fluid space between enteroids and the chamber top/bottom for volume measurement by fluorescent dye exclusion.

The dye exclusion method for measurement of enteroid volume is diagrammed in Fig. 1(b). A membrane-impermeant fluorescent dye, Alexa Fluor 647-dextran (10 kDa) was added in

the perfusate as an extracellular volume marker that did not adhere to enteroids. Enteroid swelling results in extracellular dye volume exclusion and reduced fluorescence signal in the area containing the enteroid. Using a low-magnification objective lens with wide depth-of-field, the fluorescence signal change is linear with changes in enteroid volume, allowing computation of absolute enteroid volume. This approach obviates the need for assumptions about enteroid shape changes during swelling, as needed with 2-dimensional enteroid projection or confocal images.

Microfluidic chamber characterization

As described under methods, fabrication involved two steps. A challenge in fabrication was the uniform 220–240 μm height, which required spin coating again after pre-baking. A top-view light micrograph of the trap area of the microfluidic channel in Fig. 2(a) (left) shows the arrayed post-pairs. Fig. 2(a) (right) shows top and size-view fluorescence confocal reconstructions taken of aqueous FITC (fluorescein isothiocyanate)-dextran filling the channel. The posts extended through the 240-μm high chamber.

Fig. 2(b) (left) shows a light micrograph of trapped enteroids, which, following reversal of perfusion direction, resulted in release of trapped enteroids for chamber reuse (Fig. 2(b) center and right). The solution exchange time, as judged from the integrated fluorescence intensity around enteroids, was ~3 s at a perfusion rate of 200 μl/min (Fig. 2(c)). During solution exchange the trapped enteroids remained immobilized.

Computational fluid dynamics and experimental particle tracking are useful to determine the fluid-flow pattern and shear stress in microfluidic channels.[12] The fluid-flow pattern in the microfluidic channel used here was investigated. Fig. 2(d) shows streak-lines around unoccupied post-pairs and post-pairs occupied by trapped beads. The flow pattern showed the expected

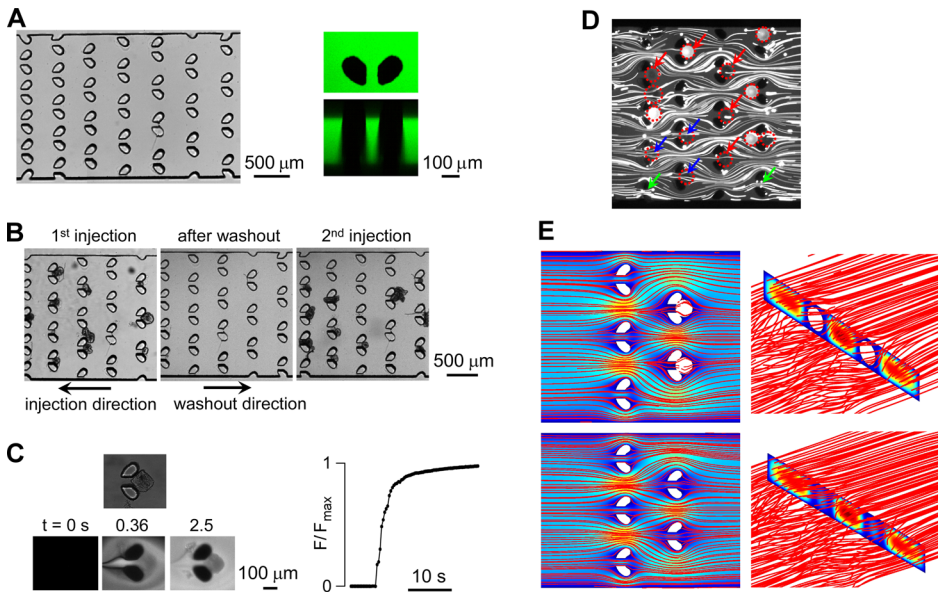

FIG. 2. Characterization of microfluidic channel. (a) Images of trap region of the channel showing top view by light microscopy (left) and top and side views by fluorescence confocal microscopy in which the channel was filled with an aqueous solution of FITC (fluorescein isothiocyanate)-dextran. (b) Release of trapped enteroids by reversal of flow direction, showing reuse with reinjection of enteroids. (c) Solution exchange time measurement around a trapped enteroid (left, top) showing fluorescence micrographs at indicated times after exchange between a non-fluorescent and fluorescent solution at a perfusion rate of 200 μl/min. Graph at right shows integrated fluorescence around the enteroid. (d) Experimental determination of streak-flow obtained by visualization of 7 μm fluorescence particles around post-pairs. (e) Three-dimensional numerical simulation using Comsol Multiphysics of flow pattern around post-pairs showing streamlines and pseudo-color velocity field in the mid-plane (left) and vertical plane (right).

deviation around trapped beads, with reduced but non-zero streak-line density through post-pairs gap (red arrows) compared with that of vacant post-pairs (green arrows). Fig. 2(e) shows computed flow streamlines without (upper) and with trapped beads (lower). The deviation in flow pattern around the bead-occupied posts was similar to that determined experimentally. The total shear stress around beads was 8.5×10^{-8} N, as determined from the computed velocity gradient and pressure.

Fig. 3(a) (and supplementary movie S2[10]) shows efficient trapping of enteroids. Injection of a heterogeneous suspension of 20–30 murine jejunal enteroids with a range of diameters from ~50 to 300 μm resulted in trapping of enteroids with diameters ~80–200 μm. The trapped enteroids remained immobilized indefinitely during perfusion. Trapping efficiency, as judged by counting the number of trapped vs. total enteroids in the trap region, was ~75% with ~15% standard deviation (Fig. 3(a), right).

Volume determination by fluorescent dye exclusion

The fluorescent dye exclusion method allows for continuous determination of absolute enteroid volume from the reduction in integrated fluorescence signal in the region extending to or beyond the boundary of each enteroid. A suitable membrane-impermeant fluorescent dye (Alexa Fluor 647-dextran, 10-kDa) and a wide depth-of-focus 2× objective lens (Nikon Plan UW) were chosen for these measurements.

Fig. 3(b) shows a light micrograph of a trapped enteroid (top) and the darkened region, or "shadow," cast by the enteroid due to fluorescent dye exclusion (bottom). The reduction in area-integrated fluorescence is a linear measure of excluded extracellular volume and hence of

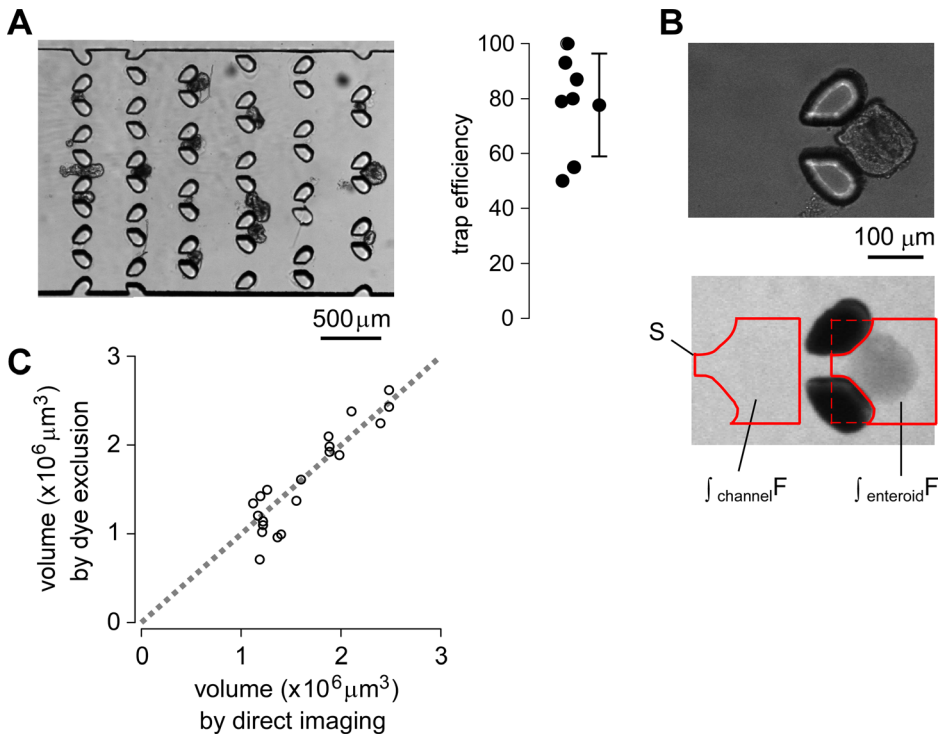

FIG. 3. Trap efficiency and volume measurement by fluorescent dye exclusion. (a) Light micrographs showing trapped enteroids (left) and deduced trap efficiency (right). For each test 20–30 enteroids with diameters of 50–300 μm were injected, and trapping efficiency was determined by counting the number of trapped vs. total enteroids in the trap region. (b) Light (top) and wide-field fluorescence (middle) micrographs obtained with 10× objective lens showing the shadow cast by dye exclusion. The fluorescence signals are integrated over indicated areas in the enteroid-occupied region and an enteroid-free region (bottom). (c) Comparison of bubble volumes determined by dye exclusion (ordinate) with actual volumes determined by light microscopy (abscissa).

enteroid volume. Enteroid volume, $V_{enteroid}$, is calculated by subtracting the enteroid-excluded volume

$$V_{enteroid} = V_{free}\left(1 - \int_{enteroid} F \Big/ \int_{free} F\right), \quad V_{free} = S \times H, \tag{1}$$

where V_{free} is the enteroid-free volume, and S is the same-size integration area for the enteroid-containing and the enteroid-free region as shown in Fig. 3(b), in which the posts are excluded by intensity threshold analysis. V_{free} is determined from S and channel height H. $\int_{enteroid}F$ is the area-integrated fluorescence over the enteroid region, and $\int_{free}F$ is the area-integrated fluorescence over the enteroid-free region. With no enteroid, $\int_{enteroid}F = \int_{free}F$, so absolute enteroid volume is zero; if an enteroid fully occupies the region, $\int_{enteroid}F$ is zero, so absolute enteroid volume is $S \times H$.

The accuracy of volume determination by dye exclusion was tested using slowly expanding air bubbles generated by injection of low-temperature (4 °C) culture media in the microchannel (see supplementary Fig. S1[10] and movie S1[10]). Bubbles were generated by sub-cooled convective boiling from the temperature differences between the injected culture media and surrounding environment.[13] Bubble volumes determined by fluorescent dye exclusion were in good agreement with those determined by light microscopic measurement of bubble diameter assuming spherical shape (Fig. 3(c)).

Enteroid swelling measurements

Two applications of the microfluidic chamber are demonstrated—osmotically and secretagogue-induced swelling. Fig. 4(a) and supplementary movie S3[10] show light microscopy

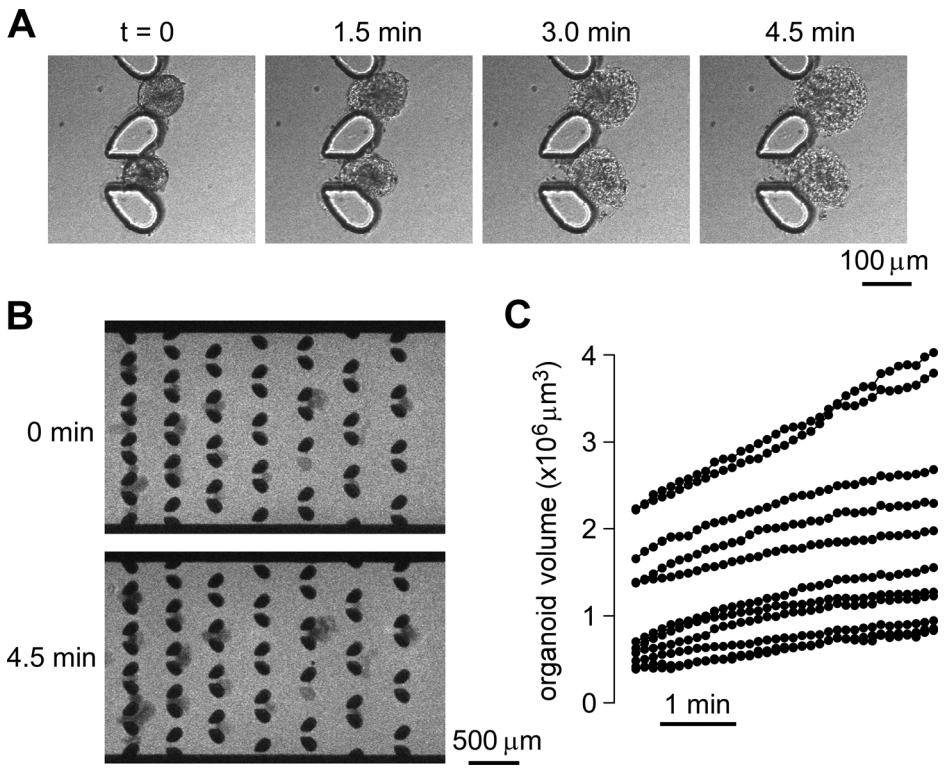

FIG. 4. Enteroid water permeability determined from measurement of osmotically induced swelling. (a) Light micrographs showing enteroid swelling at indicated times after replacement of the isosmolar bathing solution with distilled water. (b) Fluorescence micrographs of entrapped enteroids perfused with extracellular fluorescent dye before and at 4.5 min after reduced perfusate osmolality. (c) Computed kinetics of enteroid swelling following osmotic challenge.

of enteroid swelling in response to an osmotic challenge in which perfusate osmolality was reduced from 300 to 0 mOsm. As enteroids consist of tight epithelial monolayers their swelling kinetics in response to an osmotic gradient provides a quantitative measure of transcellular water transport across enterocyte cell apical and basolateral plasma membranes. Fig. 4(b) shows wide-field fluorescence micrographs of extracellular Alexa Fluor 647-dextran in response to an osmotic challenge. Alexa Fluor 647-dextran (10 μM) in the culture media was injected with the enteroids, which was followed by perfusion with distilled water containing the same concentration of fluorescent dye. Enteroid swelling reduced extracellular dye amount in the area overlying enteroids and hence the fluorescence signal.

Fig. 4(c) summarizes the deduced time course of enteroid volume following the osmotic challenge. All of the trapped enteroids of different sizes showed osmotic responses indicating an intact cell layer. From the initial swelling rates, and assuming a smooth spherical enteroid surface, the computed transepithelial osmotic water permeability coefficient (P_f) was 0.0024 ± 0.0008 cm/s (S.D.).

An important biomedical application of enteroid swelling measurements is investigation of mechanisms of secretory diarrheas and identification and testing of candidate antisecretory therapeutics. We used the microfluidic chamber to study enteroid swelling in response to cholera toxin, the major secretagogue in cholera that acts by elevation of cytoplasmic cAMP (cyclic adenosine monophosphate) and protein kinase A-mediated phosphorylation of CFTR Cl^- channels. Channel activation results in Cl^- secretion with secondary Na^+ and water transport. After trapping enteroids, cholera toxin (2 μg/100 μl in the culture media) was perfused together 10 μM Alexa Fluor 647-dextran. Fig. 5(a) (and supplementary movie S4[10]) shows light micrographs of enteroid swelling following application of cholera toxin. Figs. 5(b) and 5(c) show fluorescence micrographs of extracellular Alexa Fluor 647-dextran and deduced swelling rates. A fraction of the enteroids responded to the cholera toxin, showing a swelling response after ~1 h, with average maximum swelling rate of $\sim 8 \times 10^4$ μm^3/min. The presence of enteroids that did not respond to cholera toxin may be related to different stages of differentiation and hence CFTR expression.

DISCUSSION

The microfluidics approach developed here to follow enteroid swelling addresses an unmet need in a nascent field that has received considerable recent attention, in part because of applications of enteroid swelling assays to analyze CFTR mutations in cystic fibrosis and

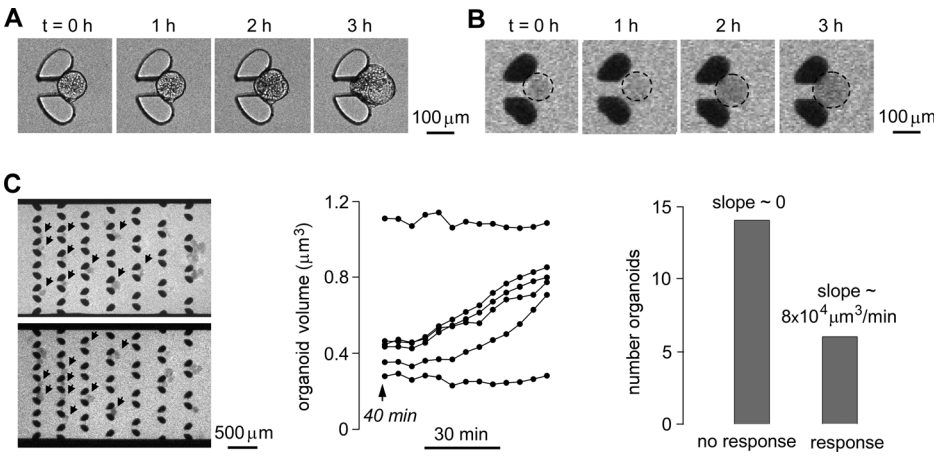

FIG. 5. Enteroid swelling in response to cholera toxin, a diarrheal secretagogue. (a) Light micrographs showing enteroid swelling at indicate times after addition of cholera toxin (2 μg/100 μl). (b) Fluorescence micrographs of extracellular Alexa Fluor 647-dextran (10 μM) following cholera toxin addition. (c) Fluorescence micrographs of multiple enteroids (left) and deduced swelling kinetics (center) in response to cholera toxin (2 μg/100 μl). (right) Number distribution of responding enteroids.

mechanisms of secretory diarrheas, as well as for drug evaluation in these diseases. Compared to the measurement method in current use, the microfluidics approach does not require a matrix to immobilize enteroids, and hence allows for rapid solution exchange with efficient solution access to the enteroid surface, and without physical restrictions on enteroid swelling. The extracellular dye exclusion method for volume measurement is simple and quantitative and does not require enteroid labeling or assumptions about enteroid shape at baseline or during swelling. The microfluidic channel design can be modified as needed to accommodate enteroids of different sizes and for parallel volume measurements on enteroid cohorts exposed to different conditions.

The heterogeneity in enteroid size and shape presented a challenge in microfluidic channel design, as large enteroids or tissue fragments could obstruct the channel, and relatively small enteroids, which are generally not suitable for swelling studies, could occupy post-pair traps or adhere to the trapped, optimal-size enteroids and preclude quantitative volume determination. In addition, efficient trapping of optimal-size enteroids was an important design criteria as the number of enteroids can be limited, for example, in preparations obtained from human intestinal biopsies.[7,11] The post-pair design and layout were optimized for efficient trapping and exclusion of small enteroids, and the pre-filter region effectively excluded large enteroids and debris. Another challenge was the measurement of absolute volume without assumptions about enteroid shape and swelling geometry, which was overcome by an extracellular dye exclusion method. A potential alternative approach, multi-slice confocal imaging of fluorescently stained enteroids, would be difficult to implement because of the large enteroid size and the need for rapid volume measurements on multiple enteroids over a greater than $\sim$1 mm^2 area. A technical challenge here was in the channel fabrication, which required a two-step spin coating process and special care during the replica molding step to prevent breakup of the deep posts.

Although this paper is the first to use a microfluidic platform to study enteroid physiology, there are prior microfluidics applications to single cell trapping,[14,15] and multi-cell trapping for culture of multicellular spheroids.[16–20] However, to date it has not been possible to form intestinal enteroids, which consist of a single layer of cells surrounding a central lumen, by trapping cells in microchannels. Culture of intestinal enteroids involves propagation of single stem cells supported in a matrix or hanging from a drop.[3–6,21] Because of this limitation, it was necessary here to use enteroids cultured in a matrix and subsequently released for trapping in the microfluidic channel. A prior study reported an electrical impedance method to measure single-cell volume changes using an on-chip electrical-impedance volume sensor with pressure-activated cell trapping capabilities.[22] Such an approach may be adaptable to enteroid volume measurements as an alternative to the optical approach used here.

The microfluidic channel was applied to measurements of osmotic and secretagogue-induced swelling of enteroids cultured from mouse jejunum. Osmotic water permeability was determined from the kinetics of enteroid swelling in response to an osmotic challenge created by reducing perfusate osmolality from 300 to 0 mOsm using the equation, $\Delta V = v_w P_f A_s \Delta Osm$, where ΔV is volume change, v_w is partial molar volume of water (18 cm^3/mol), P_f is osmotic water permeability coefficient, A_s is surface area, and ΔOsm is osmotic gradient. The P_f of 0.0024 cm/s represents the first measurement of transcellular water permeability across enterocytes, as prior measurements in intact intestine[23] are confounded by unstirred layer effects, and it has not been possible to generate primary cultures of enterocytes. The P_f of 0.0024 cm/s measured here is relatively low compared to P_f of $>$0.01 cm/s in various water-permeable epithelia where aquaporins are involved in facilitated water transport.[24] Our results support studies in the older literature where low water permeability was found in intestinal epithelial cell membrane vesicles,[25–27] where it was concluded that the intestine lacks facilitated water transport. Though there is evidence for expressions of some aquaporins on various intestinal epithelia, including aquaporins 3, 4, and 8, phenotype studies of mice lacking aquaporins have not shown significant phenotypes related to abnormal fluid transport.[28,29] The low intrinsic water permeability of the intestinal epithelium is probably sufficient to support intestinal fluid absorption and secretion, in part because of the convolved surface geometry that increases effective water permeability, and because the rates of intestinal fluid transport per unit surface area in the

intestine are low compared with those in tissues where aquaporins are needed such as in kidney tubules and salivary gland acini.

Enteroid swelling was also measured in response to cholera toxin, the major secretagogue causing secretory diarrhea in cholera. Cholera toxin causes elevation in enterocyte cAMP concentration, which, through protein kinase A, results in CFTR phosphorylation and channel activation. In intact intestine the active secretion of chloride into the lumen drives sodium and water secretion, resulting in secretory diarrhea.[30–32] The cholera toxin model is useful for testing of antisecretory compounds that affect any of these processes involved in fluid secretion. Enteroid swelling in response to other secretagogues, such as rotaviral calcium agonists, should provide useful information on enterocyte secretory mechanisms. Inhibition of enteroid swelling should be informative as an *ex vivo* surrogate to assess the antisecretory and proabsorptive action of drug candidates, and potentially applicable for phenotype-based screening to identify novel antidiarrheal targets and drug candidates.

Limitations of the microfluidics approach established here are noted. Enteroid loading into the microfluidic channel requires a matrix-free enteroid suspension and hence a non-traumatic procedure to harvest enteroids if cultured using a Matrigel matrix. Alternative culture procedures, such as growth on a collagen matrix,[33] and culture in suspension, are under development. Minimal enteroid aggregation and damage in the suspension are important, which were accomplished by using enteroids at two days after splitting and eliminating the centrifugation step during recovery from Matrigel. Though the enteroids used here from mouse jejunum were effectively trapped without trauma, channel design modifications may be necessary for use with enteroids from other tissues or species. For volume determination by extracellular dye exclusion, the dye should not bind to or permeate enteroids, or bind to the PDMS structure, and the objective lens should have sufficiently wide depth-of-focus to detect the fluorescence over the entire channel height and to minimize out-of-focus fluorescence. Last, though determination of changes in enteroid volume is not limited by the channel height, accurate determination of absolute enteroid volume is best done with uniform channel height not much greater than the maximum diameter of swollen enteroids.

CONCLUSION

The microfluidic channel designed here efficiently trapped enteroids for label-free, parallel measurement of enteroid volume during continuous perfusion. The excluded dye measurement method resolved the problem of deducing enteroid volume from projection or single-plane confocal images. Finally, the microfluidic channel implemented here is inexpensive, adaptable to different organoid/spheroid sizes and measurement protocols, and scalable for high-throughput drug discovery.

ACKNOWLEDGMENTS

This work was supported by Grant Nos. DK72517, DK35124, EY13574, EB00415, DK26523, DK61765, DK72084, DK89502, and NCATSTR00552 from the National Institutes of Health and a grant from the Cystic Fibrosis Foundation.

[1]W. Mueller-Klieser, Am. J. Physiol.: Cell Physiol. **273**, C1109 (1997).
[2]F. Pampaloni, E. G. Reynaud, and E. H. Stelzer, Nat. Rev. Mol. Cell Biol. **8**, 839 (2007).
[3]T. Sato, R. G. Vries, H. J. Snippert, M. van de Wetering, N. Barker, D. E. Stange, J. H. van Es, A. Abo, P. Kujala, P. J. Peters, and H. Clevers, Nature **459**, 262 (2009).
[4]M. K. Fuller, D. M. Faulk, N. Sundaram, N. F. Shroyer, S. J. Henning, and M. A. Helmrath, J. Surg. Res. **178**(1), 48 (2012).
[5]J. Liu, N. M. Walker, M. T. Cook, A. Ootani, and L. L. Clarke, Am. J. Physiol.: Cell Physiol. **302**(10), C1492 (2012).
[6]A. Kuratnik and C. Giardina, Biochem. Pharmacol. **85**(12), 1721 (2013).
[7]J. F. Dekkers, C. L. Wiegerinck, H. R. de Jonge, I. Bronsveld, H. M. Janssens, K. M. de Winter-de Groot, A. M. Brandsma, N. W. de Jong, M. J. Bijvelds, B. J. Scholte, E. E. Nieuwenhuis, S. van den Brink, H. Clevers, C. K. van der Ent, S. Middendorp, and J. M. Beekman, Nat. Med. **19**, 939 (2013).
[8]G. Schwank, B. K. Koo, V. Sasselli, J. F. Dekkers, I. Heo, T. Demircan, N. Sasaki, S. Boymans, E. Cuppen, C. K. van der Ent, E. E. Nieuwenhuis, J. M. Beekman, and H. Clevers, Cell Stem Cell **13**(6), 653 (2013).
[9]J. R. Thiagarajah and A. S. Verkman, Clin. Pharmacol. Ther. **92**, 287 (2012).

[10]See supplementary material at http://dx.doi.org/10.1063/1.4870400 for supporting figure and movies.
[11]T. Sato, D. E. Stange, M. Ferrante, R. G. Vries, J. H. Van Es, S. Van den Brink, W. J. Van Houdt, A. Pronk, J. Van Gorp, P. D. Siersema, and H. Clevers, Gastroenterology **141**, 1762 (2011).
[12]F. Shen, X. Li, and P. C. H. Li, Biomicrofluidics **8**, 014109 (2014).
[13]S.-S. Hsieh and C.-Y. Lin, J. Micromech. Microeng. **20**, 015027 (2010).
[14]D. D. Carlo, L. Y. Wu, and L. P. Lee, Lab Chip **6**, 1445 (2006).
[15]X. Y. Peng and P. C. H. Li, Lab Chip **5**, 1298 (2005).
[16]A. Khademhosseini, G. Eng, J. Yeh, P. A. Kucharczyk, R. Langer, G. Vunjak-Novakovic, and M. Radisic, Biomed. Microdevices **9**, 149 (2007).
[17]L. Y. Wu, D. D. Carlo, and L. P. Lee, Biomed. Microdevices **10**, 197 (2008).
[18]L. Yu, M. C. W. Chen, and K. C. Cheung, Lab Chip **10**, 2424 (2010).
[19]B. Patra, Y.-H. Chen, C.-C. Peng, S.-C. Lin, C.-H. Lee, and Y.-C. Tung, Biomicrofluidics **7**, 054114 (2013).
[20]H.-J. Jin, Y.-H. Cho, J.-M. Gu, J. Kim, and Y.-S. Oh, Lab Chip **11**, 115 (2011).
[21]T. Sato and H. Clevers, Science **340**, 1190 (2013).
[22]J. Riordon, M. Nash, W. Jing, and M. Godin, Biomicrofluidics **8**, 011101 (2014).
[23]J. R. Thiagarajah and A. S. Verkman, in *Physiology of the Gastrointestinal Tract*, edited by L. R. Johnson, F. Ghishan, J. Kaunitz, J. Manchant, H. Said, and J. Wood (Elsevier, New York, 2012), Vol. 5, p. 1757.
[24]A. S. Verkman, Annu. Rev. Med. **63**, 303 (2012).
[25]M. P. van Heeswijk and C. H. van Os, J. Membr. Biol. **92**(2), 183 (1986).
[26]H. J. Worman and M. Field, J. Membr. Biol. **87**(3), 233 (1985).
[27]J. A. Dempster, A. N. van Hoek, M. D. de Jong, and C. H. van Os, Pflugers Arch. **419**(3–4), 249 (1991).
[28]K. S. Wang, T. Ma, F. Filiz, A. S. Verkman, and J. A. Bastidas, Am. J. Physiol. Gastrointest. Liver Physiol. **279**(2), G463 (2000).
[29]B. Yang, Y. Song, D. Zhao, and A. S. Verkman, Am. J. Physiol.: Cell Physiol. **288**(5), C1161 (2005).
[30]S. E. Gabriel, K. N. Brigman, B. H. Koller, R. C. Boucher, and M. J. Stutts, Science **266**, 107 (1994).
[31]K. E. Barrett and S. J. Keely, Annu. Rev. Physiol. **62**, 535 (2000).
[32]J. R. Thiagarajah, T. Broadbent, E. Hsieh, and A. S. Verkman, Gastroenterology **126**, 511 (2004).
[33]Z. Jabaji, C. M. Sears, G. J. Brinkley, N. Y. Lei, V. S. Joshi, J. Wang, M. Lewis, M. Stelzner, M. G. Martín, and J. C. Dunn, Tissue Eng., Part C **19**(12), 961 (2013).